ELSEVIER

Materials Science and Engineering A 402 (2005) 250–257

MATERIALS SCIENCE & ENGINEERING A

www.elsevier.com/locate/msea

Relationship between texture and low temperature superplasticity in an extruded AZ31 Mg alloy processed by ECAP

H.K. Lin [a], J.C. Huang [a,*], T.G. Langdon [b]

[a] *Institute of Materials Science and Engineering, Center for Nanoscience and Nanotechnology, National Sun Yat-Sen University, Kaohsiung, Taiwan 804, ROC*

[b] *Departments of Aerospace & Mechanical Engineering and Materials Science, University of Southern California, Los Angeles, CA 90089-1453, USA*

Received 22 November 2004; received in revised form 7 April 2005; accepted 7 April 2005

Abstract

The development of low temperature superplasticity and texture is examined in an AZ31 Mg alloy after extrusion and processing by equal-channel angular pressing (ECAP). It is demonstrated that an elongation of ~460% may be attained at a temperature of 150 °C, equivalent to 0.46 T_m where T_m is the absolute melting temperature. This result demonstrates the potential for achieving low temperature superplasticity. The experimental results show that the mechanical properties of the alloy are influenced by the different textures present after extrusion and after extrusion and subsequent processing by ECAP.

Keywords: Equal-channel angular pressing; Extrusion; Magnesium; Superplasticity; Texture

1. Introduction

The increasing shortage of natural resources, together with the world-wide implementation of stricter environmental regulations, is making it necessary to produce and utilize a range of light-weight metallic alloys for the transportation industry. Magnesium is currently the lightest metal in use for structural applications. However, whereas there has been a steady growth in the use of magnesium in the electronics industry, due primarily to the need for light-weight parts for laptop computers and consumer electronic products [1], there has been no parallel growth in other industries. This lack of growth is a direct consequence of the poor workability of magnesium alloys because of their hexagonal close-packed (HCP) crystal structure and the consequent limitation on the number of available slip systems. In addition, magnesium alloys are attractive for use in a future hydrogen economy since magnesium is the only metallic element capable of reversibly storing a high volume of hydrogen in the form of metal hydrides. Accordingly, the present investigation was motivated by the need to significantly improve the workability of magnesium-based alloys and to thereby develop a viable forming technology.

Equal-channel angular pressing (ECAP) was used to process a magnesium alloy where this procedure was selected for three reasons. First, ECAP is a processing technique involving the application of severe plastic deformation (SPD) and it is well established that SPD techniques are capable of producing fully-dense bulk solids having ultrafine grain sizes [2]. Second, it is known that alloys with ultrafine grain sizes may exhibit superplasticity both at high strain rates (HSRSP, defined as superplasticity at strain rates at or above 10^{-2} s^{-1} [3]) and/or at low temperatures (LTSP, defined as superplasticity at temperatures below 0.5 T_m where T_m is the absolute melting temperature) and significant success has been reported to date in using ECAP with aluminum-based alloys to achieve HSRSP [4–18] and LTSP [19–21]. Third, it was demonstrated recently that the hydrogen desorption rate is higher in a magnesium ZK60 alloy after ECAP processing than in the same alloy processed using conventional high-

* Corresponding author. Tel.: +886 7 525 2000x4063; fax: +886 7 525 4099.
E-mail address: jacobc@mail.nsysu.edu.tw (J.C. Huang).

0921-5093/$ – see front matter © 2005 Elsevier B.V. All rights reserved.
doi:10.1016/j.msea.2005.04.018

Table 1
Summary of high ductilities in Mg alloys after ECAP processing

Alloy (wt.%)	Grain size (μm)	T (°C)	$\dot{\varepsilon}$ (s^{-1})	ε (%)	Ref.
AZ91	0.7	200	6.2×10^{-5}	661	[23–25]
ZK60	1.4	200	1×10^{-5}	1083	[26,27]
Mg–9Al	0.7	200	3.3×10^{-4}	840	[28]
Mg–10Li–1Zn	–	150	1×10^{-3}	391	[29]
Mg–0.6Zr	1	300	3.3×10^{-4}	420	[30]
Mg–0.6Zr	1.4	300	3.3×10^{-4}	380	[31]

energy ball-milling [22], thereby suggesting that ECAP may represent a promising processing technique for the future development of new hydrogen storage materials.

There have been limited reports of high ductilities achieved in Mg alloys using ECAP, as summarized in Table 1 where $\dot{\varepsilon}$ is the strain rate and ε is the elongation to failure [23–31]. However, inspection shows that, although some of the elongations are very high (for example, 1083% in ZK60 [26]), none of the alloys exhibits HSRSP and, except only for one report [29], the testing temperatures are consistently at or above 200 °C equivalent to ∼0.51 to 0.54 T_m. The present investigation was therefore initiated to evaluate the potential for using ECAP to achieve LTSP in an magnesium AZ31 alloy where AZ31 was selected because earlier work demonstrated the occurrence of superplastic elongations in this alloy when testing in the extruded condition without ECAP [32,33].

2. Experimental material and procedures

An AZ31 alloy with a composition, in wt.%, of Mg-3% Al-1% Zn-0.3% Mn was obtained from the CDN Company, Delta, BC, Canada. The as-received alloy was produced through semi-continuous casting and provided in the form of an extruded billet measuring 178 mm in diameter and 300 mm in length. The grain size in the cast condition was ∼75 μm.

The as-received billets were initially extruded at 300 °C using an extrusion ratio of 42:1 to give rods with diameters of 10 mm. Henceforth, these bars are termed the extruded condition. Some of the extruded rods were then processed by ECAP at 200 °C for eight passes using a die with an internal angle of 110° between the two channels and an angle of 20° at the outer arc of curvature where the two channels intersect. Processing was performed using route B_c [34] where the samples are rotated by 90° in the same direction between each pass. It can be shown from first principles that the accumulative true strain after 8 passes is ∼6 [35]. The bars processed by extrusion and ECAP are termed the ECAP condition.

Tensile tests were conducted at constant cross-head speeds using an Instron 5582 universal testing machine equipped with a three-zone furnace. The temperature was controlled to within ±2 °C and the tests were conducted within the temperature range from 150 to 250 °C using initial strain rates from 10^{-4} to 10^{-2} s^{-1}. The tensile specimens had gauge lengths and diameters of 8.3 and 4.0 mm, respectively, and the specimens were machined so that the loading directions were parallel to the extrusion or pressing directions.

The grain structures were examined by optical microscopy (OM) and transmission electron microscopy (TEM). X-ray diffraction (XRD) and electron back-scatter diffraction (EBSD) were used to examine the transverse cross-sectional planes of the as-received billets and samples in the extruded and ECAP conditions. The areas examined by XRD and EBSD were approximately 10 mm × 10 mm and 600 μm^2, respectively. Several separate areas were selected for the construction of EBSD pole figures in order to ensure good reproducibility.

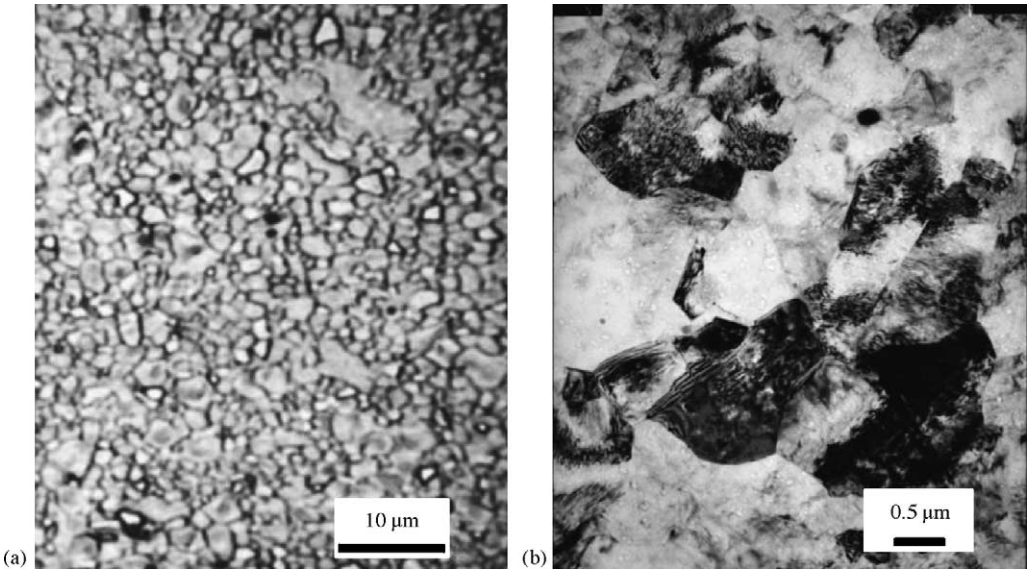

Fig. 1. Grain structure micrographs of the AZ31 alloy after (a) extrusion at 300 °C (OM micrograph) and (b) ECAP at 200 °C (TEM micrograph).

3. Experimental results

3.1. Microstructures in the extruded and ECAP conditions

Fig. 1 shows the grain structures of the AZ31 alloy in (a) the extruded and (b) the ECAP conditions, respectively. Both conditions yielded arrays of essentially equiaxed grains and the grain sizes measured using the linear intercept method were ∼2.5 and ∼0.7 μm for these two conditions, respectively, these results are given in the top row of Table 2.

The thermal stability of the grains was examined by heating samples at temperatures up to 350 °C and statically annealing for a period of 1 h: the results from the static annealing are shown in Fig. 2. It is apparent that reasonable grain stability is maintained up to 200 °C for the ECAP condition but with pronounced grain growth at higher temperatures, whereas the extruded condition shows reasonable grain stability up to a temperature of 300 °C.

3.2. Tensile testing of specimens in the as-received, extruded and ECAP conditions

Typical stress–strain curves are shown in Fig. 3 for tests conducted at room temperature at an initial strain rate of $1.0 \times 10^{-3}\,s^{-1}$ using samples in the as-received, extruded and ECAP conditions: the values of the tensile yield stress (YS), the ultimate tensile stress (UTS) and the elongation to failure are summarized for these three conditions in Table 2.

Table 2
Grain size and room temperature tensile properties of the billet, extruded and ECAP specimens

	Billet	Extruded	ECAP
Grain size (μm)	75	2.5	0.7
YS (MPa)	100	265	217
UTS (MPa)	160	319	282
Elongation (%)	9	28	30

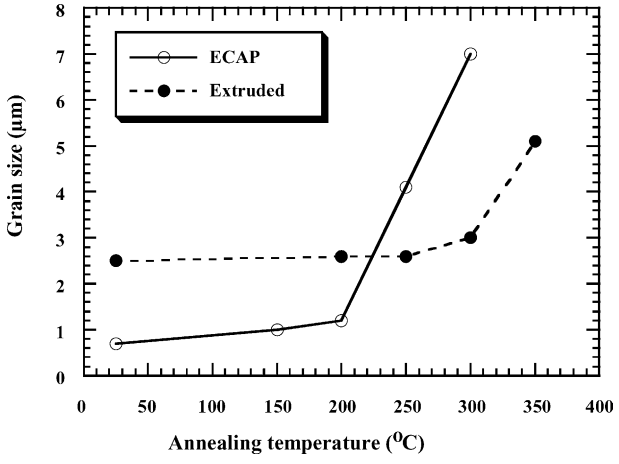

Fig. 2. Grain size vs. annealing temperature after static annealing of the extruded and ECAP samples.

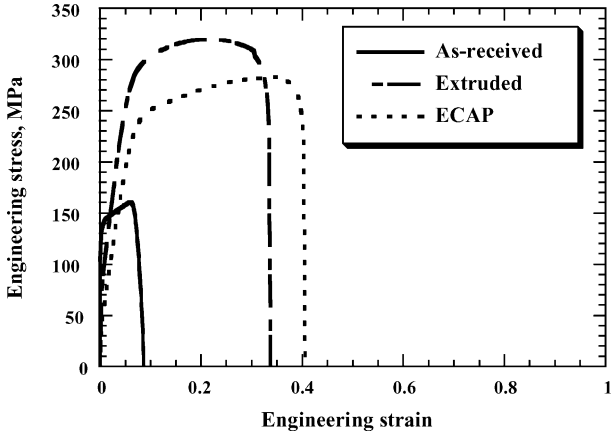

Fig. 3. Typical room temperature stress–strain curves for the as-received, extruded and ECAP conditions.

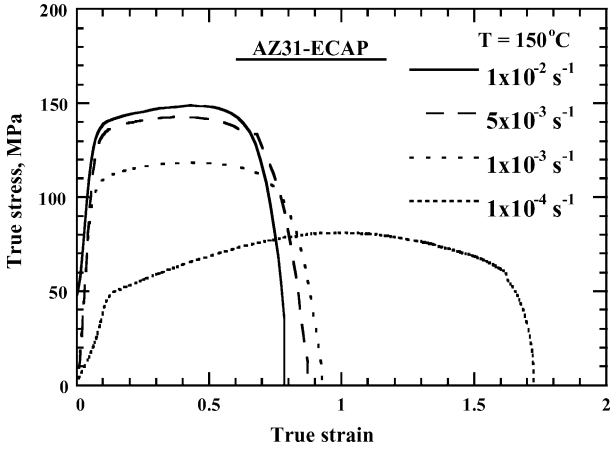

Fig. 4. Plots of true stress vs. true strain at 150 °C for samples processed by ECAP for 8 passes at 200 °C.

Although the grain size is smallest in the ECAP condition, it is important to note that the YS and UTS are lower in the ECAP condition than in the extruded condition although the ECAP condition yields values of YS and UTS, which are significantly higher than in the as-received billet.

Fig. 4 shows typical plots of true stress versus true strain for tests conducted on the ECAP material at 150 °C, equivalent to ∼0.46 T_m. The highest elongation achieved under these conditions was ∼460% at a strain rate of $1.0 \times 10^{-4}\,s^{-1}$ for a specimen showing a region of extensive strain hardening. A full summary of all of the tensile elongations is given in Fig. 5 where the results are plotted against the testing strain rate at three different testing temperatures for (a) the extruded condition and (b) the ECAP condition. In Fig. 5(a) for the extruded condition, reasonably high elongations occur only at a testing temperature of 250 °C. By contrast, it is apparent from Fig. 5(b) that superplasticity is achieved in the ECAP condition at the lowest strain rate when testing at a temperature of 150 °C. It is apparent from inspection of Fig. 2 that the low elongations recorded in Fig. 5(b) for the ECAP condition at 250 °C are a direct consequence of the extensive grain growth

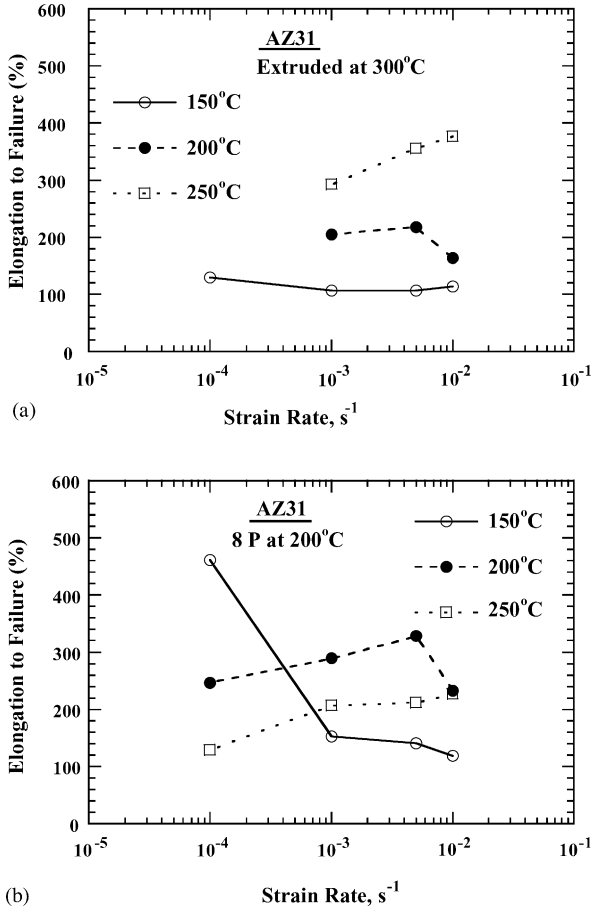

Fig. 5. Elongation vs. strain rate at 150–250 °C for (a) the extruded and (b) the ECAP conditions.

occurring at this temperature so that the submicrometer grain size is removed. Thus, measurements showed that the average grain sizes in the gauge sections of the ECAP specimens strained to failure at a strain rate of $1.0 \times 10^{-4}\,s^{-1}$ at 150, 200 and 250 °C were ~1, ~3 and ~8 μm, respectively.

3.3. Texture characterization

Fig. 6(a) shows the X-ray diffraction pattern simulated by computer for random Mg powders and Fig. 6(b) and (c) show the patterns taken from the transverse cross-sectional planes of samples in the extruded and ECAP conditions, respectively. It is apparent by inspection that the $\{1\,0\,\bar{1}\,0\}$ planes for the extruded specimens show a strong tendency to lie perpendicular to the extrusion axis but this trend has been lost in the ECAP condition. The X-ray (0 0 0 2), $(1\,0\,\bar{1}\,0)$ and $(1\,0\,\bar{1}\,1)$ pole figures are given in the three rows in Fig. 7 for the extruded condition (on left) and the ECAP condition (on right): it should be noted that, in order to protect the X-ray detector, only the poles within 0–80° were constructed. It is apparent from Fig. 7, in confirmation with the X-ray diffraction patterns shown in Fig. 6, that most of the $\{1\,0\,\bar{1}\,0\}$ planes in the extruded condition lie perpendicular to the extrusion axis

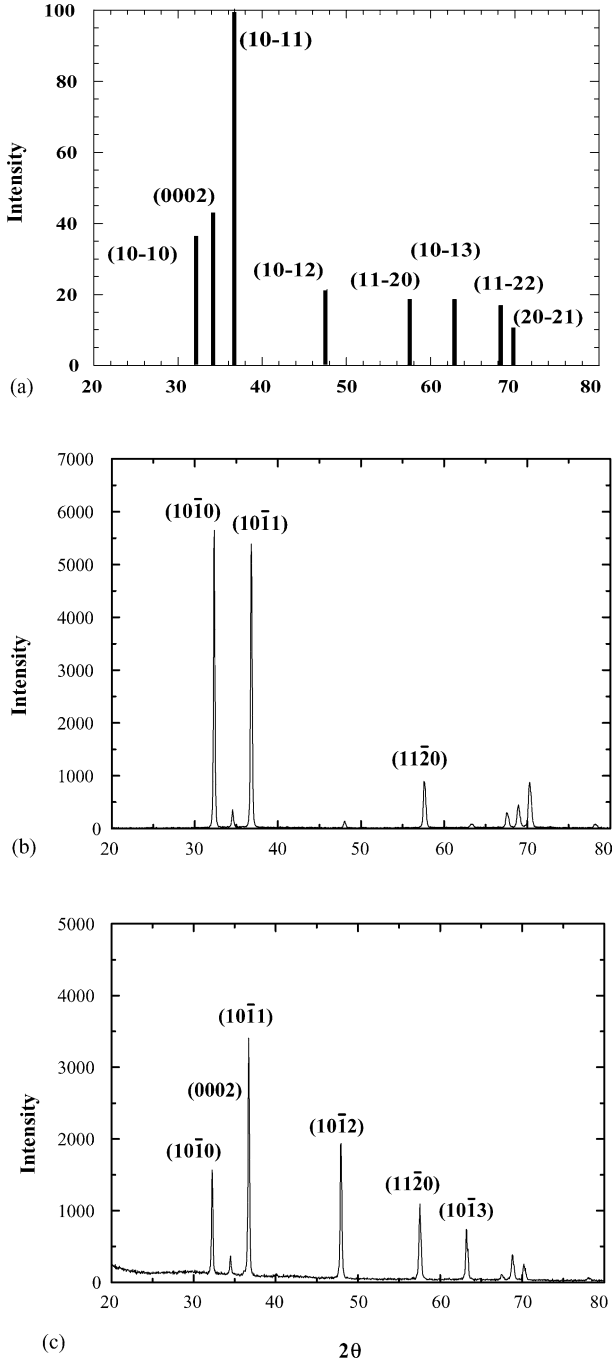

Fig. 6. X-ray diffraction patterns for (a) the random pure Mg powders, (b) the transverse cross-sectional plane in the extruded condition and (c) the transverse cross-sectional plane in the ECAP condition.

and it follows therefore that the (0 0 0 2) planes generally lie parallel to the extrusion axis. By contrast, the (0 0 0 2) basal planes in the ECAP condition lie primarily within an angular range from 40° to 50° with respect to the pressing direction (or with respect to the normal direction, ND, assigned in the pole figures). Since ECAP processing was undertaken in this investigation using a die with a channel angle of 110°, it is reasonable to anticipate that the basal planes in the majority of grains will rearrange during processing to become close

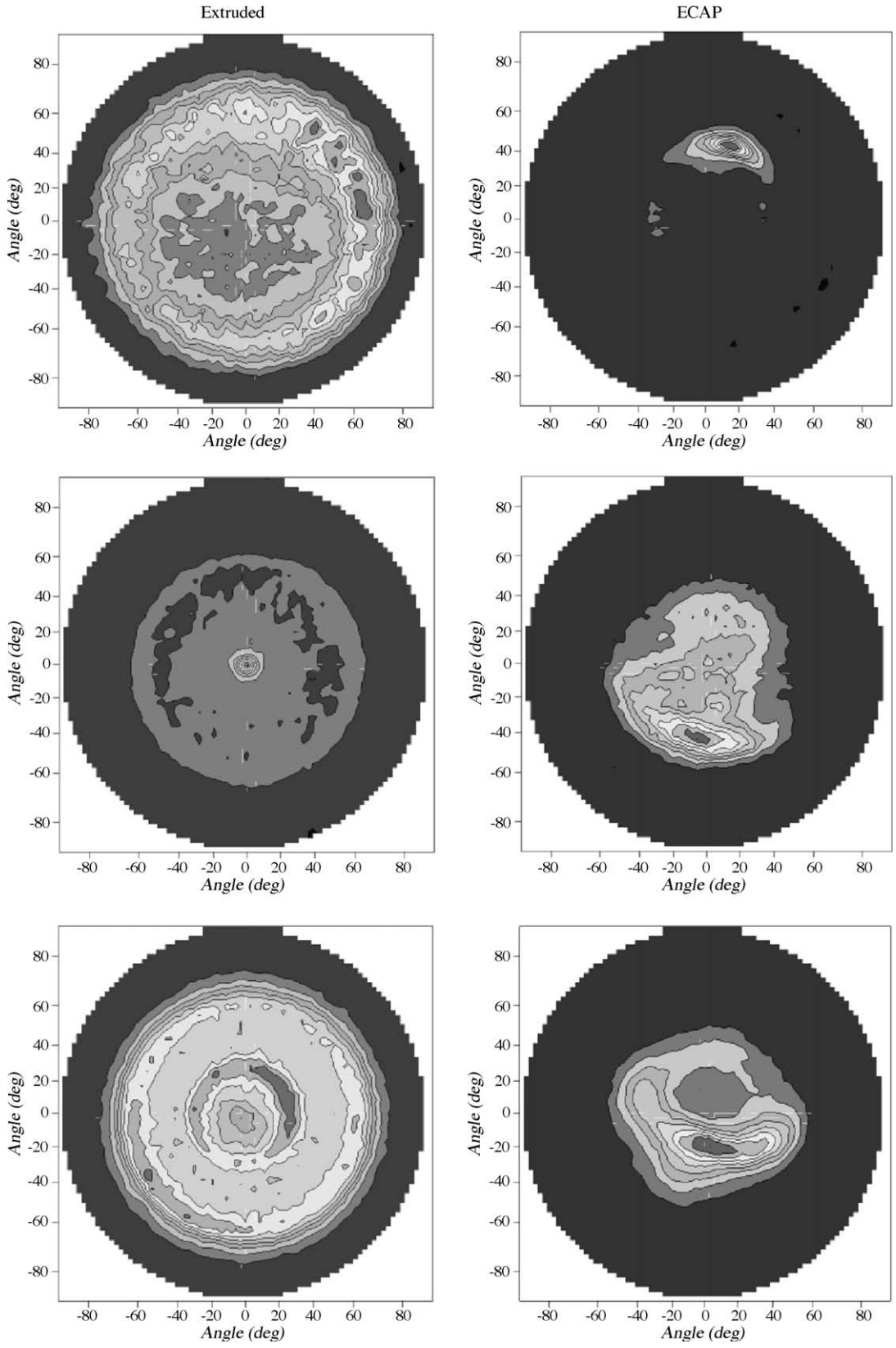

Fig. 7. The X-ray (0 0 0 2), (1 0 $\bar{1}$ 0) and (1 0 $\bar{1}$ $\bar{1}$) pole figures for the extruded and ECAP conditions.

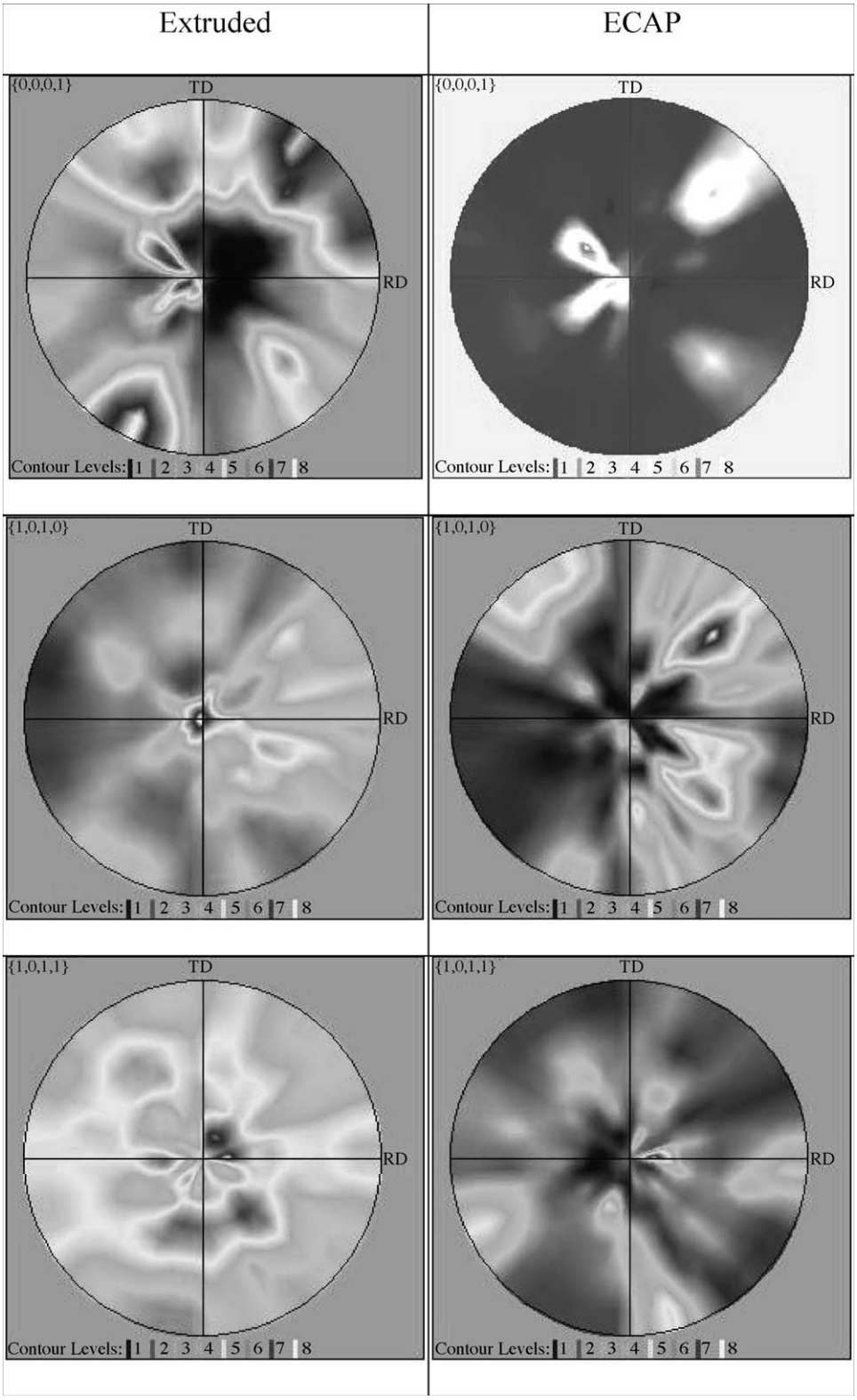

Fig. 8. The EBSD (0 0 0 2), (1 0 $\bar{1}$ 0) and (1 0 $\bar{1}$ $\bar{1}$) pole figures for the extruded and ECAP conditions.

to the theoretical shearing plane as the billet passes through the die.

Parallel pole figures were also constructed by EBSD for some local regions on the transverse cross-sectional planes in the extruded and ECAP conditions and these are shown in the two columns in Fig. 8. These EBSD results are generally consistent with the X-ray pole figures and the diffraction patterns, thereby providing additional confirmation of the overall conclusions.

4. Discussion

These experiments confirm the potential for achieving LTSP in the AZ31 alloy through processing using a combination of extrusion and ECAP. This two-step procedure of extrusion and ECAP, designated earlier as EX-ECAP [28], is effective in producing significant grain refinement in magnesium-based alloys whereas experiments have shown that ECAP conducted without any preliminary extrusion leads only to a relatively minor grain refinement in Mg alloys: for example, the grain size of a cast Mg-0.9% Al alloy was reduced only from an initial value of ~100 to ~17 μm through ECAP at 200 °C so that an ultrafine submicrometer grain size was not achieved [36]. In the present experiments, the grain size was reduced from ~75 μm in the as-received cast condition to ~2.5 μm through extrusion and then to ~0.7 μm through subsequent processing by ECAP. This reduction is sufficient to produce LTSP, which is absent in the extruded condition. A maximum elongation of ~460% was achieved after extrusion and ECAP when testing at a strain rate of $1.0 \times 10^{-4}\,s^{-1}$ at a temperature of 150 °C. This temperature is equivalent to 0.46 T_m and it is within the range generally associated with LTSP. As shown in Table 1, the present result compares favorably with the report of an elongation of 391% for a Mg-10% Li-1% Zn alloy also tested under the same conditions of temperature and strain rate [29].

Based on the texture characterization, the nature of the microstructures for the extruded and ECAP conditions may be illustrated schematically by depicting the predominant grain orientations for these two conditions, as shown in Fig. 9 where the arrows at right indicate the tensile axes for the subsequent the tensile testing. The results for the extruded condition are consistent with earlier reports demonstrating an alignment of the basal planes into the extrusion direction in various Mg alloys [32,37–39]. It is reasonable also to anticipate that these different types of texture will impose an influence on the room and low temperature stress–strain curves for the extruded and ECAP conditions. This effect is clearly documented in Fig. 3 where the preferred orientation of the basal planes in the ECAP condition, and the consequent easier slip in tensile testing, leads to lower values of the YS and the UTS by comparison with the extruded condition despite the presence of a smaller grain size after ECAP.

It is possible to check this conclusion quantitatively using the stereographic projections for pure Mg. Thus, it follows that <1 0 $\bar{1}$ 0>//ED and <$\bar{2}$ $\bar{5}$ 7 6>//ED correspond to the extruded and ECAP conditions, respectively, where ED is the extrusion direction. Considering the three primary slip systems in hexagonal structures, namely (i) the basal {0 0 0 1}<1 1 $\bar{2}$ 0>, (ii) the prismatic {1 0 $\bar{1}$ 0}<1 1 $\bar{2}$ 0> and (iii) the pyramidal {1 0 $\bar{1}$ 1}<1 1 $\bar{2}$ 0> slip systems, it follows that the average Schmid factors may be calculated for each system as summarized in Table 3. These calculations confirm there is a high Schmid factor of 0.27 for basal {0 0 0 1}<1 1 $\bar{2}$ 0> slip in the ECAP condition whereas the Schmid factor is zero for the extruded condition. The calculations are therefore consistent with the lower YS and higher elongation observed for the ECAP condition at room temperature and 150 °C when dislocation slip is the rate-controlling deformation process. By contrast, at the higher temperature of 250 °C, as documented in Fig. 5, the influence of this more favorable texture is lost in the ECAP condition because of the occurrence of significant grain growth.

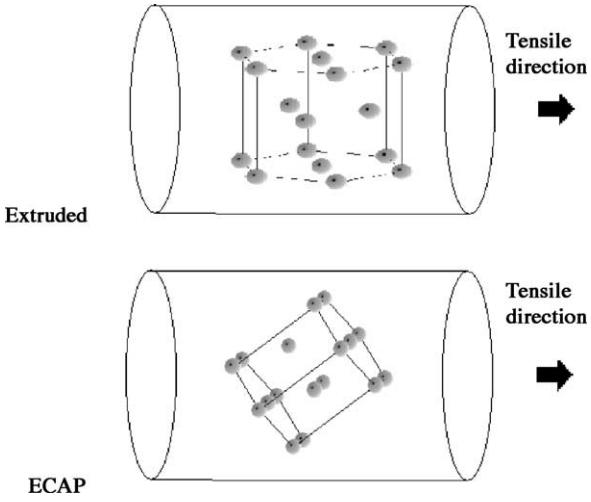

Fig. 9. Schematic illustration of the dominant textures in the extruded and ECAP conditions.

Table 3
Schmid factors calculated for extruded and ECAP specimens

Sample	Texture	Slip system	Average schmid factor
Extruded	<1 0 $\bar{1}$ 0>//ED	{0 0 0 1}<1 1 $\bar{2}$ 0>	0
		{1 0 $\bar{1}$ 0}<1 1 $\bar{2}$ 0>	0.29
		{1 0 $\bar{1}$ 1}<1 1 $\bar{2}$ 0>	0.25
ECAP	<$\bar{2}$ $\bar{5}$ 7 6>//ED	{0 0 0 1}<1 1 $\bar{2}$ 0>	0.27
		{1 0 $\bar{1}$ 0}<1 1 $\bar{2}$ 0>	0.14
		{1 0 $\bar{1}$ 1}<1 1 $\bar{2}$ 0>	0.11

5. Summary and conclusions

1. The grain size of the AZ31 alloy was reduced from ~75 μm in the as-received condition to ~2.5 μm by a single-pass extrusion at 300 °C and to ~0.7 μm through additionally processing by ECAP for 8 passes at 200 °C. Following extrusion and ECAP, the AZ31 alloy exhib-

ited low temperature superplasticity (LTSP) with a maximum elongation of ~460% when using a strain rate of $1.0 \times 10^{-4}\,s^{-1}$ at 150 °C, equivalent to a homologous temperature of $0.46\,T_m$.

2. A detailed investigation revealed different textures in the extruded and ECAP conditions. These dominant textures were characteristic of <1 0 $\bar{1}$ 0>//ED in the extruded condition and <$\bar{2}$ $\bar{5}$ 7 6>//ED in the ECAP condition, where ED is the extrusion direction. The results show that the basal planes tend to lie parallel to the extrusion axis in the extruded condition but there is a rearrangement during ECAP and the basal planes become reasonably aligned with the theoretical shearing plane.
3. Using the measured textures and the calculated Schmid factors, it is anticipated that the ECAP specimens will exhibit lower yield stresses and higher elongations to failure at room temperature when dislocation slip is the dominant rate-controlling process. This is consistent with the experimental observations.

Acknowledgements

One of the authors (HKL) gratefully acknowledges support under the Ph.D. Student Exchange Program sponsored by the National Science Council of ROC under Project no. NSC 92-2917-I-110-003. This research was sponsored by Project no. NSC 91-2216-E-110-006.

References

[1] A.A. Lou, JOM 54 (2) (2002) 42.
[2] R.Z. Valiev, R.K. Islamgaliev, I.V. Alexandrov, Prog. Mater. Sci. 45 (2000) 102.
[3] K. Higashi, M. Mabuchi, T.G. Langdon, ISIJ Int. 36 (1996) 1423.
[4] R.Z. Valiev, D.A. Salimonenko, N.K. Tsenev, P.B. Berbon, T.G. Langdon, Scripta Mater. 37 (1997) 1945.
[5] S. Komura, P.B. Berbon, M. Furukawa, Z. Horita, M. Nemoto, T.G. Langdon, Scripta Mater. 38 (1998) 1851.
[6] S. Lee, P.B. Berbon, M. Furukawa, Z. Horita, M. Nemoto, N.K. Tsenev, R.Z. Valiev, T.G. Langdon, Mater. Sci. Eng. A272 (1999) 63.
[7] Z. Horita, M. Furukawa, M. Nemoto, A.J. Barnes, T.G. Langdon, Acta Mater. 48 (2000) 3633.
[8] S. Komura, Z. Horita, M. Furukawa, M. Nemoto, T.G. Langdon, J. Mater. Res. 15 (2000) 2571.
[9] S. Komura, Z. Horita, M. Furukawa, M. Nemoto, T.G. Langdon, Metall. Mater. Trans. 32A (2001) 707.
[10] S. Komura, M. Furukawa, Z. Horita, M. Nemoto, T.G. Langdon, Mater. Sci. Eng. A297 (2001) 111.
[11] S. Lee, A. Utsunomiya, H. Akamatsu, K. Neishi, M. Furukawa, Z. Horita, T.G. Langdon, Acta Mater. 50 (2002) 553.
[12] C. Xu, M. Furukawa, Z. Horita, T.G. Langdon, Acta Mater. 51 (2004) 6139.
[13] K.-T. Park, D.-Y. Hwang, Y.-K. Lee, Y.-K. Kim, D.H. Shin, Mater. Sci. Eng. A341 (2003) 273.
[14] S. Lee, M. Furukawa, Z. Horita, T.G. Langdon, Mater. Sci. Eng. A342 (2003) 294.
[15] R.K. Islamgaliev, N.F. Yunusova, R.Z. Valiev, N.K. Tsenev, V.N. Perevezentsev, T.G. Langdon, Scripta Mater. 49 (2003) 467.
[16] D.H. Shin, D.-Y. Hwang, Y.-J. Oh, K.-T. Park, Metall. Mater. Trans. 35A (2004) 825.
[17] F. Musin, R. Kaibyshev, Y. Motohashi, G. Itoh, Metall. Mater. Trans. 35A (2004) 2383.
[18] F. Musin, R. Kaibyshev, Y. Motohashi, G. Itoh, Scripta Mater. 50 (2004) 511.
[19] K.-T. Park, D.-Y. Hwang, S.-Y. Chang, D.H. Shin, Metall. Mater. Trans. 33A (2002) 2859.
[20] W.J. Kim, J.K. Kim, T.Y. Park, S.I. Hong, D.I. Kim, Y.S. Kim, J.D. Lee, Metall. Mater. Trans. 33A (2002) 3155.
[21] K.-T. Park, S.-H. Myung, D.H. Shin, C.S. Lee, Mater. Sci. Eng. A371 (2004) 178.
[22] V.M. Skripnyuk, E. Rabkin, Y. Estrin, R. Lapovok, Acta Mater. 52 (2004) 405.
[23] M. Mabuchi, H. Iwasaki, K. Higashi, Mater. Sci. Forum 243–245 (1997) 547.
[24] M. Mabuchi, M. Nakamura, K. Ameyama, H. Iwasaki, K. Higashi, Mater. Sci. Forum 304–306 (1999) 67.
[25] M. Mabuchi, K. Ameyama, H. Iwasaki, K. Higashi, Acta Mater. 47 (1999) 2047.
[26] H. Watanabe, T. Mukai, K. Ishikawa, K. Higashi, Scripta Mater. 46 (2002) 851.
[27] H. Watanabe, T. Mukai, K. Ishikawa, K. Higashi, Mater. Sci. Forum 419–4232 (2003) 557.
[28] K. Matsubara, Y. Miyahara, Z. Horita, T.G. Langdon, Acta Mater. 51 (2003) 3037.
[29] Y. Yoshida, L. Cisar, S. Kamado, Y. Kojima, Mater. Trans. 43 (2002) 2419.
[30] Z. Horita, K. Matsubara, K. Makisi, T.G. Langdon, Scripta Mater. 47 (2002) 255.
[31] K. Matsubara, Y. Miyahara, Z. Horita, T.G. Langdon, Metall. Mater. Trans. 35A (2004) 1735.
[32] H.K. Lin, J.C. Huang, Mater. Trans. 43 (2002) 2424.
[33] C.J. Lee, J.C. Huang, Acta Mater. 52 (2004) 3111.
[34] M. Furukawa, Y. Iwahashi, Z. Horita, M. Nemoto, T.G. Langdon, Mater. Sci. Eng. A257 (1998) 328.
[35] Y. Iwahashi, J. Wang, Z. Horita, M. Nemoto, T.G. Langdon, Scripta Mater. 35 (1996) 143.
[36] A. Yamashita, Z. Horita, T.G. Langdon, Mater. Sci. Eng. A300 (2001) 142.
[37] D.V. Wilson, J. Inst. Metals 98 (1970) 133.
[38] M. Hilpert, A. Styczynski, J. Kiese, L. Wagner, in: B.L. Mordike, K.U. Kainer (Eds.), Magnesium Alloys and Their Applications, Wiley-VCH, Weinheim, Germany, 1998, p. 319.
[39] T. Mukai, M. Yamanoi, H. Watanabe, K. Higashi, Scripta Mater. 45 (2001) 89.